NASA CR- 175279

Lockheed Missiles & Space Company, Inc.
RESEARCH AND DEVELOPMENT • PALO ALTO, CALIFORNIA

D/197

ULTRAVIOLET SPECTROMETER AND POLARIMETER (UVSP) SOFTWARE DEVELOPMENT AND HARDWARE TESTS FOR THE SOLAR MAXIMUM MISSION

Interim Report

1 July - 30 September, 1984

Contract NAS5-24119

M.E. Bruner, Project Leader
B.M. Haisch

Lockheed Palo Alto Research Laboratory
3251 Hanover Street
Palo Alto, California 94304

CONTRACT REPORT FOR NAS5-24119
Period 1 July, 1984 - 30 Sept, 1984

Work on the contract during this period has included an analysis of UVSP wavelength drive hardware, problems, and recovery procedures; a continuation of the study with Dr. McWhirter on radiative power loss from solar plasmas; editorial work on chapter 5 for the forthcoming book on results of the SMM workshop; and a study of correlations between observed UV brightness and inferred photospheric currents.

UVSP WAVELENGTH DRIVE PROBLEM ANALYSIS (M. Bruner)

During M. Bruner's visit to GSFC in Sept, 1984, a meeting was convened to review the problems that had been experienced with the wavelength drive following the successful SMM Repair Mission in April. Initial investigations, carried out by resident UVSP technical team members had indicated that the wavelength drive was not responding to step commands, either from "Jr", the instrument computer, or from the redundant mode electronics. Indications for this conclusion were twofold: that the wavelength drive null indication was not received when the motor was commanded to step through a complete revolution, and that the balance of observed signal between the two detectors of an exit slit pair did not change as a result of the attempted motion. An earlier attempt to switch to a redundant set of motor drive electronics had also failed to restore proper operation.

Plans for diagnostic tests on the system began with the definition of fault isolation test sequences designed to distinguish between three possibilities: 1) that the motor driver electronics were not receiving step pulses from the Experiment Logic Unit (ELU); 2) that the pulses were being received, but the drive motor electronics were not working properly; and 3) that the pulses were being received, the drive motor electronics were functioning properly, but the motor was not turning because of mechanical interference. Differential diagnosis was to be based on observation of the experiment quiet bus current, which would reflect the motor current pulses. If the current pulses were observed to be of the predicted size, then the fault would have been mechanical; if not, then the problem was in the electronics.

As a first step in preparing the differential diagnostic test procedure, a detailed review of the motor drive electronics was conducted by M. Bruner and K. Meese (GSFC). H. Tinsley from SCI Systems R. Rehse from Lockheed, and personnel from GSFC and General Electric participated in later phases of the study. The results of this review are summarized in the following points:

1. The motor pulse width is determined by external commanding, not by the motor drive circuit.

2. The 5 volt logic power for the motor drive unit must be ON in order to successfully command the unit to switch between redundant drive electronics sections.

3. There is no status indicator to show which driver is in use.

4. The "Select B Driver" command is a toggle function. That is; the first command sent transfers from the A driver to the B driver, the next one transfers back to A, and so forth. There is no way to force a desired state if the current state is unknown.

5. The state of the A/B select logic is retained in the latching relay K1 (on GE drawing number 47J242875), when the motor driver is powered down. The circuits are correctly initialized when power is restored.

6. The flip-flop U3 (same drawing) on board A2 holds power off the motor windings for a short time at the beginning of each step in order to allow all switching levels to change. This delay prevents a possible switching transient mode in which 28 V power could be connected directly to ground for a brief period while changing from one step position to the next. U3 does not control the motor pulse length.

7. All four motor windings operate all the time, increasing the original (OSO 8) motor torque rating by a factor of the square root of 2.

8. A failure mode in which one winding failed open would probably not prevent the motor from operating, though the steps would no longer be equal in size. There would be two large ones and two small ones. Motor winding current would be 2/3 of the value that would be normal if all four windings were drawing current. This situation is illustrated schematically in Figure 1.

9. A failure mode in which one switching transistor failed open would probably not prevent the motor from operating and the steps would be of different sizes. In this case, one step would be larger than normal, two smaller, and one of normal size. The current would differ from step to step, with two being low (around 2/3 normal) and two normal. This case is shown in Figure 2.

10. The stable position of the motor rotor when the windings are powered up is 45 degrees in phase away from the magnetic detent in the unpowered state. This phase angle offset corresponds to a 45/12 = 3.75 degree shaft angle offset.

Point 2, above was in conflict with existing 'lore' about the motor driver operation, which was that the command to transfer between the redundant halves of the drive electronics would operate with the 5 volt logic power either ON or OFF. During all previous attempts to transfer to the redundant drive electronics, the 5 volt power had been turned OFF in order to prevent an undesirable change in the wavelength drive position indicated by the ELU. This, of course, prevented the transfer from occurring, as noted above.

In view of the earlier misconception, it was decided to make another attempt to transfer to the redundant motor drive unit before proceeding with the differential diagnostic tests. This attempt succeeded, as subsequent

tests of the wavelength drive motor demonstrated.

The first test of the drive following the successful transfer was carried out under control of the ELU only, rather than under "Jr" program control. Indications of correct functioning included the observation of three "null" signals (which occur once per revolution of the motor shaft), and a change in the balance between the signal levels observed with the two detectors.

Figure 3 is a composite plot showing the response of the two detectors to a short spectrum scan done during the first attempt to operate the drive under "Jr" control. The experiment was carried out with 3 A wide exit slits, which had been in use for UVSP work during the previous several weeks. The record showed that there were two fairly narrow lines in the long wavelength exit slit, as the signal level dropped in two distinct stages as the spectrum was scanned. The line widths and separations can be estimated from these curves by considering them as integral functions of the line profiles that would have been seen if very narrow slits had been used. This analysis showed that the line pair was separated by about 1.17 A, and that the full width at half maximum was about 0.15 A for the longer wavelength line.

A search of the solar spectrum atlas showed two candidate line pairs; the C II doublet at 1334.532 and 1335.708 A (1.18 A separation), and the long wavelength pair of the O I triplet at 1304.58 and 1306.02 A (1.16 A separation). Lines at much longer wavelengths were ruled out by the low level of the observed continuum. Figure 4 shows the next wavelength scan, also made under "Jr" control, in which a smaller slit width was used. Indicated on the figure is the location where the 1302.18 line of O I would be located if the others were due to oxygen. The line is clearly absent, showing that the observed pair is properly identified as the C II doublet. Subsequent spectral scans confirmed this identification.

Operation of the wavelength drive system since the successful transfer has appeared to be normal, and highly reliable. We point out, however, that until differential diagnostic tests including measurements of the individual step currents have been run, the actual state of the hardware remains unknown. In light of the results of the motor driver review, particularly points 8 and 9, it is a distinct possibility that the system is now operating in a partially failed mode. If this is the case, it should be recognized and taken into account in the planning of future operations. We therfore strongly recommend that differential diagnostic studies be carried out, both on the existing data base, and on the hardware in its present configuration. It is our belief that these studies can be carried out without either risk to the hardware or investment of a major manpower effort. Lockheed will be pleased to participate in the definition and conduction of these studies.

RADIATED POWER STUDY (M. Bruner and R. W. P. McWhirter)

Efforts on the radiated power study centered on expansion of the atomic physics data base to incorporate additional ions and transitions, and to extend the temperature range. SOL procedures were written to subdivide tables using cubic spline interpolation, and to assemble data files for processing by the radiated power code. These codes were delivered to GSFC in

September and successfully installed and run on the XRP PDP-11 computer. A series of runs on various differential emission measure models failed to confirm an earlier result that indicated that the ratio of the power in transition zone lines to the total radiated power appeared to be insensitive to the form of the model.

IMAGE CORRELATION STUDIES (B. M. Haisch)

The question of the heating of the solar corona (and stellar coronae) is equivalent to the question of what heats individual magnetic structures in the outer solar atmosphere; the long-held hypothesis that sound waves were directly responsible for heating the corona is thus no longer in favor simply because the highly structured nature of the outer solar atmosphere by magnetic fields appears to be inconsistent with a uniform or a randomly distributed global heating process. Moreover it is also the case that the net acoustic wave energy flux has now been measured, and it appears from this measurement that the acoustic wave energy flux is some three orders of magnitude below the required flux to maintain the solar corona and the solar wind (Bruner 1981).

The alternative to acoustic heating is magnetic heating; this in turn may be magnetic heating due to dissipation of magnetic waves (cf. Priest 1982), or it may be heating resulting from dissipation of electric currents. Heating of coronal plasma by current dissipation has been investigated by (among others) Tucker (1973) and Rosner et al. (1978). The physical process dominating the dissipation is unclear; it may be simple ohmic heating or it may be dissipation dominated by plasma turbulence.

Spicer (1983) has pointed out that any current densities giving rise to coronal heating must already exist at the photospheric boundary, and in fact the currents probably originate in the convection zone; Hinata (1983) shows that even a rather weak current density (i. e. a J too weak to account for coronal heating) can supply a considerable amount of heating at the temperature minimum and chromospheric level. Thus although it is likely to be acoustic waves that are the dominant source of chromospheric heating, it makes sense to search for evidence of magnetic heating deriving from current dissipation at the temperature mimimum and chromospheric level.

Recently deLoach et al. (1984) compared inferred electric current densities with SMM UVSP maps of an active region in Lyman-alpha and in N V; they did find a rough correspondence between Jz and a minor enhancement in Lyman-alpha and N V emission. We have co-registered the Lyman-alpha images with the 1600 A images for the 23 September 1980 rocket data set and based on the plage topology have coregistered with that longitudinal and transverse magnetic field magnetograms from the MSFC vector magnetograph. A C IV UVSP raster map has been examined; the spatial resolution of the C IV image is in 3 arc-sec pixels. There is an excellent correspondence between the general outline of plage emissions and between the network emissions in C IV and Lyman-alpha; this correspondence has been used to coregister the C IV map with the Lyman-alpha image, and from that the neutral line has been identified with respect to C IV. We have intercompared the inferred regions of current density vis-a-vis the brightest emission areas in Lyman-alpha and C IV respectively. Unfortunately there appears to be no significant correlation of inferred electric current with enhanced emission in either Lyman-alpha or C IV.

FIGURES

As a cost saving measure, the figures for this report have been reproduced directly from notes or working prints, rather than from new artwork.

Figure 1. Open Winding Failure Mode.

The four coils of each drawing represent the four windings of the wavelength drive motor. Each drawing represents the power configuration for one of a series of four consecutive motor steps. In the top drawing, for example, + 28 volts is applied to the top winding while the right and bottom windings are connected to ground. The left winding is presumed to have failed, and is an open circuit. Each winding has a resistance of R, so that the total resistance is 1.5 R and the net current is I=V/1.5R. All three coils will contribute to the resultant magnetic field, whose phase with respect to the four windings is represented by the arrow. The dashed line represents the phase of the resultant field in the normal case (no failure) where all four coils are carrying current and contributing to the resultant field. In the actual motor there are twelve sets of poles, so that this phase diagram is repeated twelve times around the periphery of the motor pole piece. It is seen from the set of diagrams, that successive step pulses will always cause the phase to advance, so that the motor will run, though the size of the steps will be uneven. Vector analysis of the phase diagram shows that the first and third steps will be 45 degrees in phase, while the second and fourth will be 135 degrees. The corresponding motor shaft motions will be 45/12 = 3.75 degrees and 135/12 = 11.25 degrees, respectively.

Figure 2. Open Switching Transistor Failure Mode

In these diagrams, we illustrate the effect of an open failure in one of the switching transistors. We have assumed that the transistor that switches the left coil to ground has failed in an open condition. In this case, the motor current is normal for two of the four steps, and 2/3 of normal for the other two. The resultant phases of the magnetic field vector are shown by arrows as before. Here again, the phase always advances at each step, so that the motor will run. The step sizes (in degrees of phase) will be 67.5, 135, 67.5, and 135 degrees, respectively.

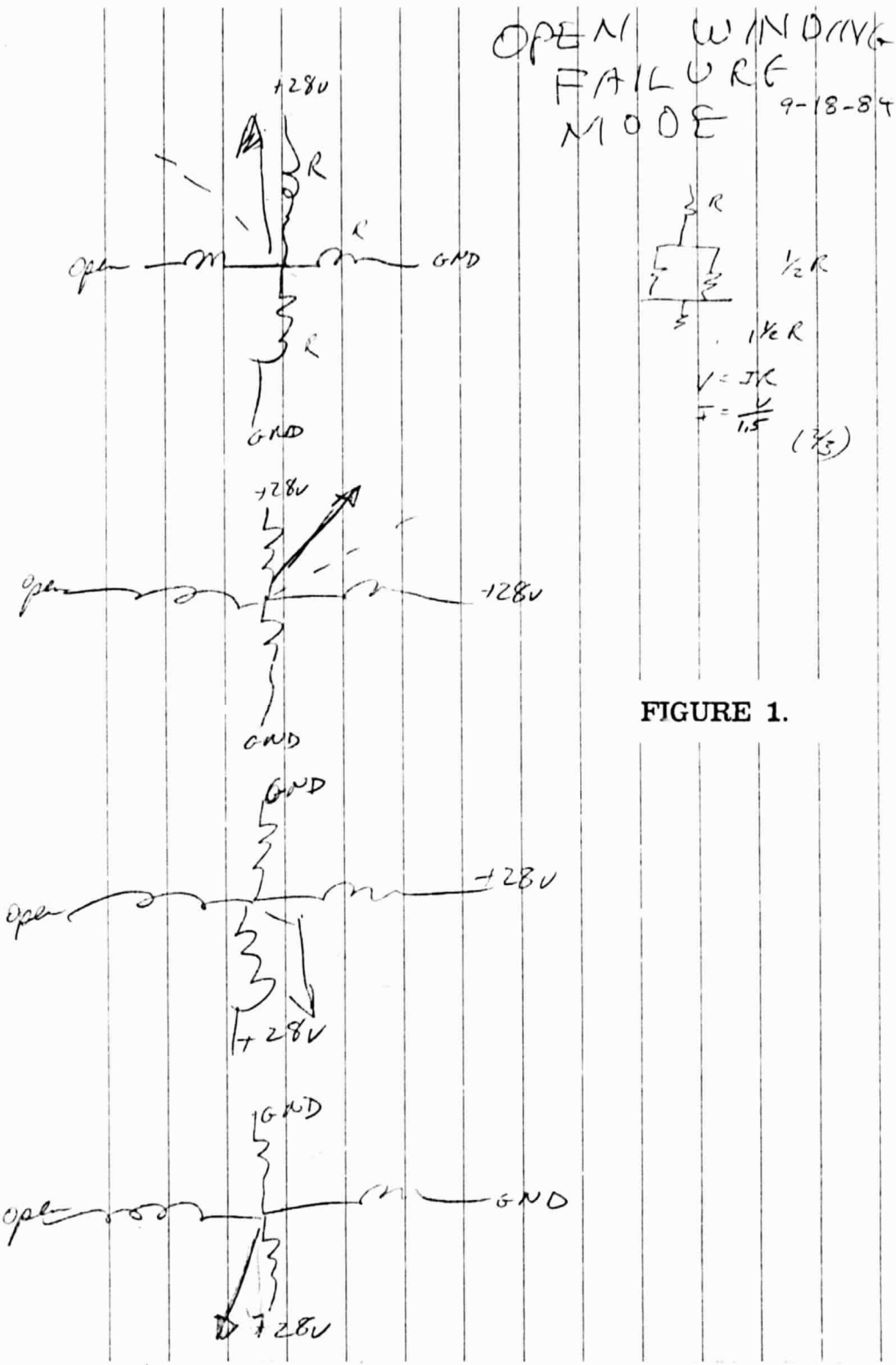

FIGURE 1.

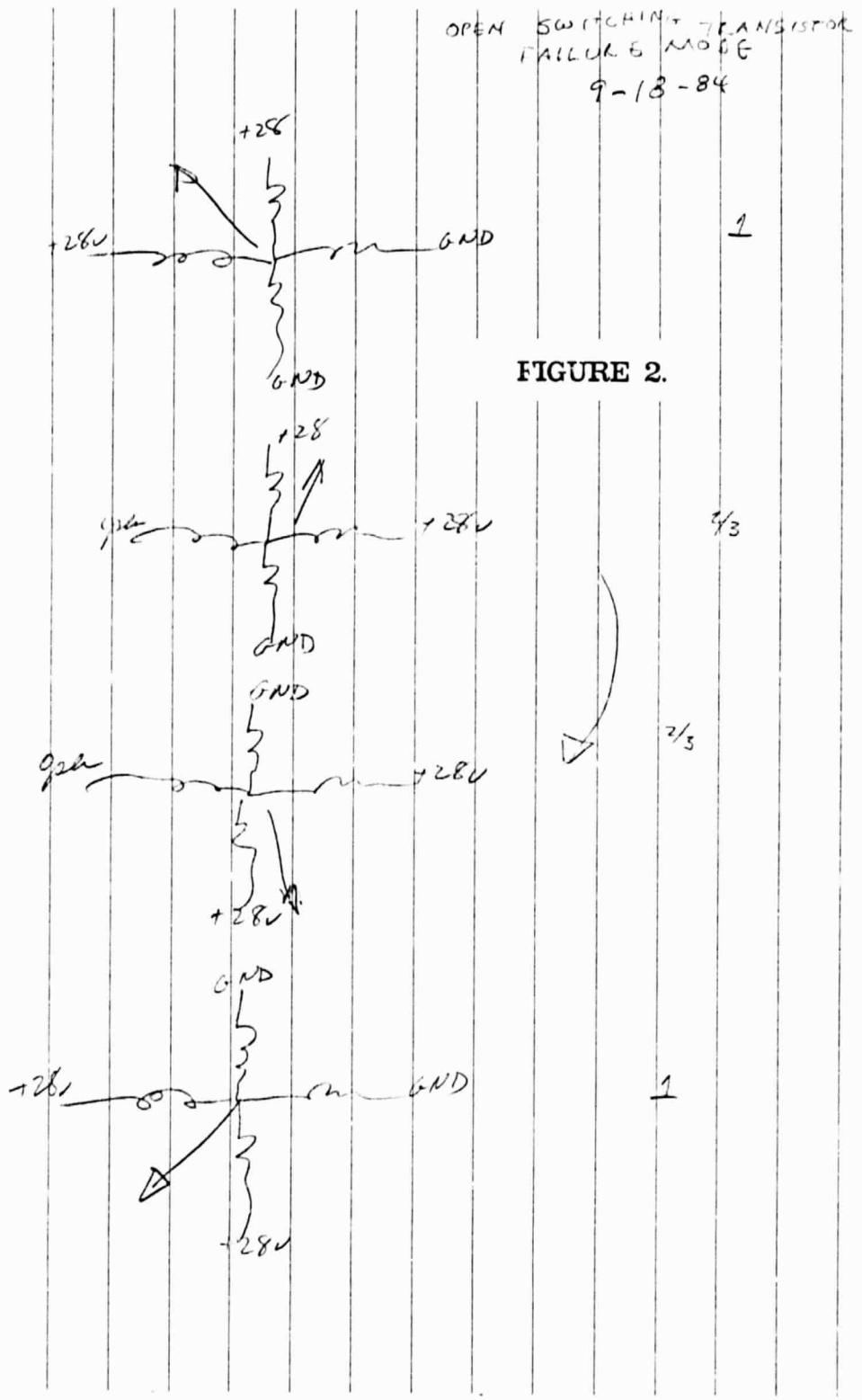

FIGURE 2.

Figure 3. Wavelength Drive Position Analysis I

This diagram shows how the first successful "Jr." controlled experiment following recovery was analyzed to determine the wavelength drive position. The upper curve represents the observed count rate as a function of wavelength for the long wavelength slit. The lower curve is that for the short wavelength slit. The upper curve falls toward the background level in two distinct stages; the first at about 0.75 Angstroms, and the second at about 1.8 Angstroms. This shows that the portion of the spectrum being observed contained two distinct lines. The separation between the two "half power" points gives the separation of the lines, while the distance between 3/4 and 1/4 power points for the long wavelength component gives its full width at half maximum. The results were consistent with either the C II doublet at 1335 A or the long wavelength pair of the O I triplet at 1302, 1305, and 1306 A.

Figure 4. Wavelength Drive Position Analysis II

This figure shows where the 1302.18 line would have been located if the line pair inferred from Figure 3 had been due to the O I triplet. Its absence demonstrates that the lines were due to the C II doublet.

9-18-84
Record of 1st successful
Jr Experiment moving wavelength line

721-0986

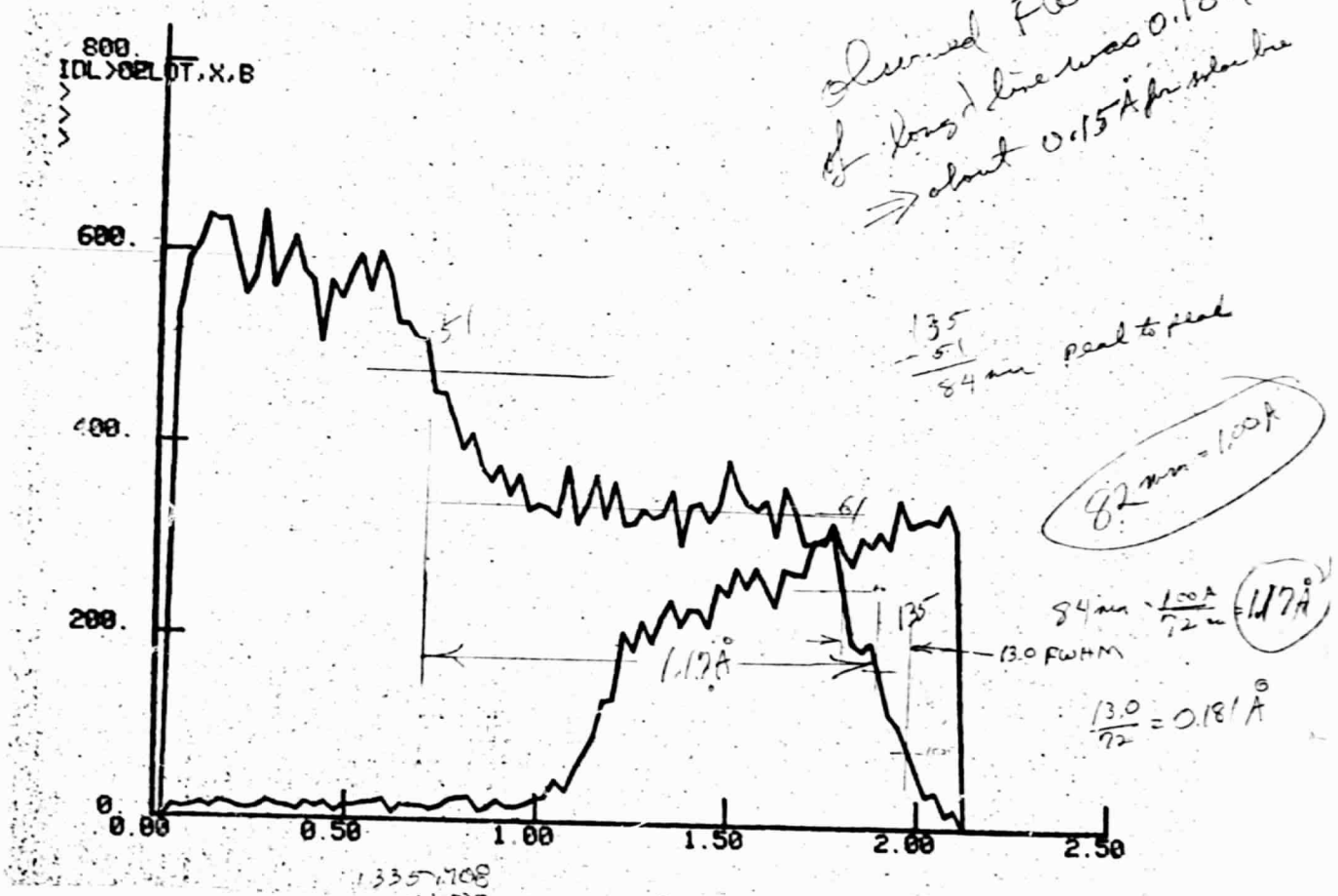

Observed FWHM of long line was 0.181 Å
⇒ about 0.15 Å for short line

135 − 51 = 84 mm peak to peak

82 mm = 1.00 Å

84 mm · 1.00 Å / 72 mm = 1.17 Å

13.0 / 72 = 0.181 Å

1335.708
1334.532
C II ⇒ 1.18 Å

O I 1304.858 − 1306.02 ⇒ 1.16 Å

deconvolving a 0.1 Å gaussian ⇒ 0.149 Å FWHM Lorentz

FIGURE 3.

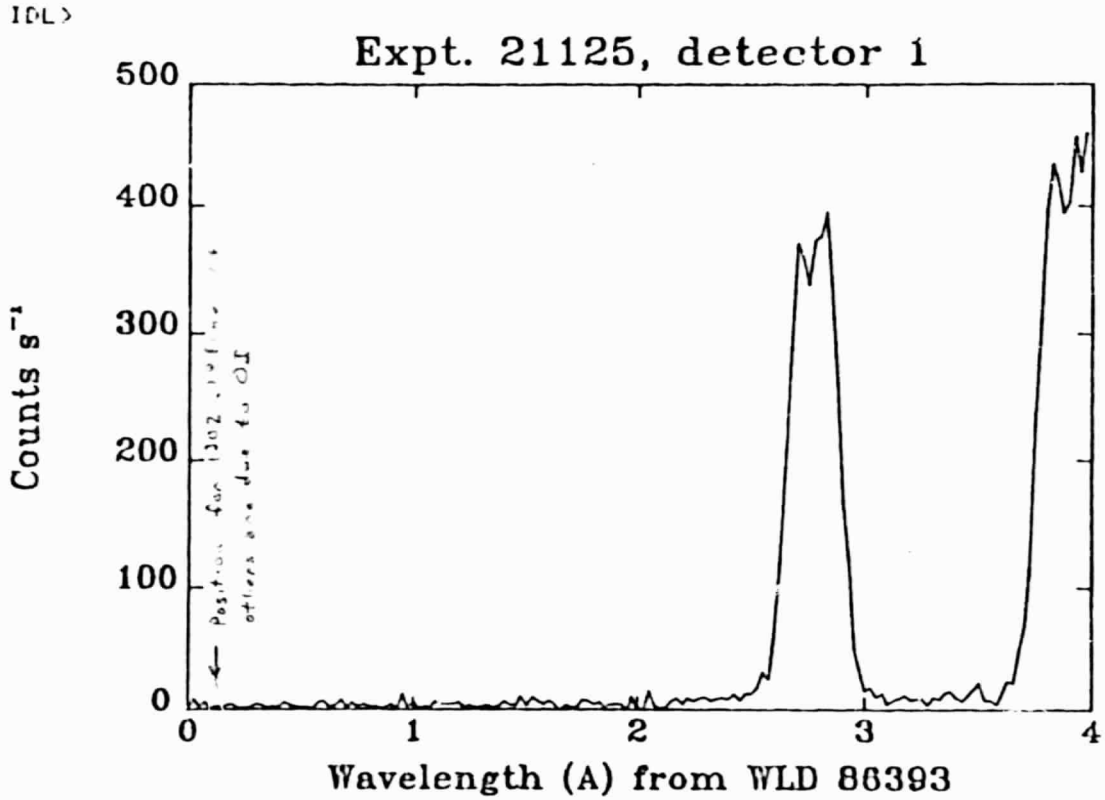
Expt. 21125, detector 1
500
400
300
200
100
0
Counts s⁻¹
0
1
2
3
4
Wavelength (A) from WLD 86393

FIGURE 4.